



MOBILITY OF A SEMI-INFINITE BEAM WITH CONSTANT CURVATURE

S. J. WALSH

*Department of Aeronautical and Automotive Engineering and Transport Studies,
Loughborough University, Loughborough LE11 3TU, England*

AND

R. G. WHITE

*Department of Aeronautics and Astronautics, University of Southampton,
Southampton SO17 1BJ, England*

(Received 27 April 1998, and in final form 13 November 1998)

In a straight beam the flexural and longitudinal wave motions are uncoupled. For a curved beam, however, there is interaction between the longitudinal and bending deformations leading to coupled extensional–flexural wave propagation. In this paper coupled extensional–flexural wave propagation is investigated by considering the mobility of a “semi-infinite” beam with a constant radius of curvature. Both theoretical and experimental results are discussed and formulae for the point and cross mobilities of the structure are presented.

© 1999 Academic Press

1. INTRODUCTION

In the design stage of a vehicle there is often a need to predict the vibration transmission to the structure by an applied force. One design method is based upon using formulae for the mobility of simple structural elements. Many useful formulae have already been published for structural elements such as beams, plates and rings. In this paper simple design formulae are sought to describe the mobility of a “semi-infinite” beam where the centre line forms a plane of constant radius of curvature. The cross-section of the beam is uniform and symmetrical about the plane and it is assumed that there is no motion perpendicular to the plane. It is also assumed that the beam material is linearly elastic, homogenous, isotropic and continuous.

There have been a number of previous studies of the wave motion in a curved beam. In an elementary theory by Love [1] it is assumed that the centre-line remains unextended during flexural motion, whilst flexural behaviour is ignored when considering extensional motion. Using these assumptions the vibrational behaviour of complete or incomplete rings has been considered by many researchers who are interested in the low frequency behaviour of arches and reinforcing rings [2]. In the same reference [1] Love presented equations for thin

shells which include the effects of extension of the mid-surface during bending motion. Flügge [3] has also derived equations for thin shells which include extension of the mid-surface during bending motion but which are more consistent when discarding higher order terms. Both these sets of equations can be reduced to equations applicable to a curved beam. Equations derived specifically for a curved beam are presented by Philipson [4] who included extension of the central line in the flexural wave motion, and also rotary inertia effects. In a development analogous to that of Timoshenko for straight beams, Morley [5] introduced a correction for radial shear when considering the vibration of curved beams. Graff later presented frequency versus wave number and wave speed versus wave number data for wave motion in a curved beam, for the Love based equations [6], and when including higher order effects [7].

However, dispersion curves only describe the possible types of wave motion in the structure: no assumptions are made about any excitation force or boundary conditions. In the present work the vibrational response of a curved “semi-infinite” beam when excited at its free end by a purely circumferential force is developed by considering the propagating and evanescent waves in the beam. This method has previously been used to analyse the flexural response of a straight Euler–Bernoulli beam on periodic [8] and non-periodic supports [9]. To validate the theoretical predictions, experimental studies were undertaken on a curved mild steel beam with a constant radius of curvature. In section 3 the apparatus used for these experiments is described and the measurement method outlined. In section 4 a comparison between the measured and predicted mobilities is presented which leads to a set of simple formulae for the point and cross mobilities of the structure.

2. THEORY

2.1. BEAM EQUATIONS AND FREE WAVE SOLUTION

Consider a portion of a curved beam, as shown in Figure 1. The circumferential co-ordinate measured around the centre-line is s , while the outward pointing normal co-ordinate from the centre-line is z , and the general radial co-ordinate is r . The centre-line is defined as the locus of centroids of each cross-sectional element. The tangential and radial displacements of a material point are $U(r, s, t)$ and $W(r, s, t)$ respectively. For small displacements of thin beams the assumptions known as “Love’s first approximation” [3], in classical shell theory, can be made which leads to the following linear relationships between the displacements of a material point and components of displacement at the undeformed centre-line:

$$U(r, s, t) = u(R, s, t) + z\phi(s, t), \quad (1)$$

$$W(r, s, t) = w(R, s, t), \quad (2)$$

where u and w are the components of displacement at the centre-line in the tangential and radial directions, respectively, and ϕ is the rotation of the normal

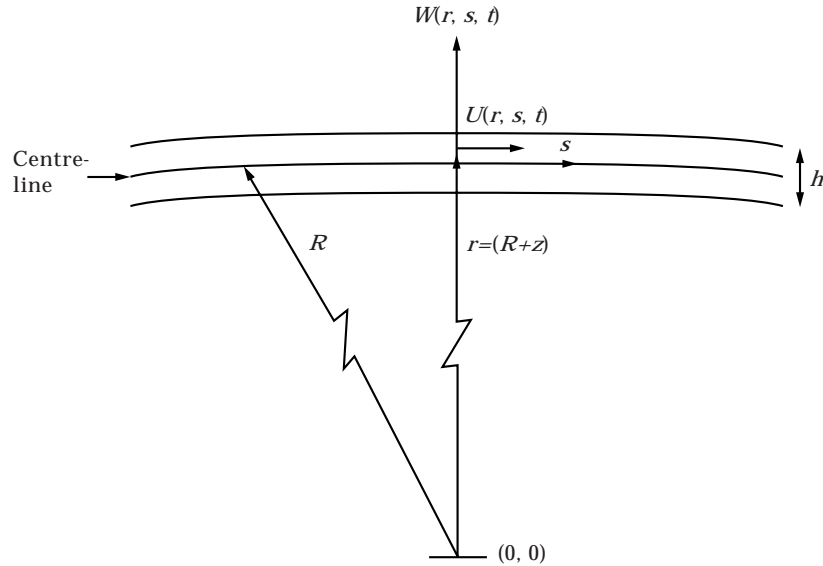


Figure 1. Geometry of a curved beam.

to the centre-line during deformation:

$$\phi = \underbrace{\frac{u}{R}}_{\text{(angle of curvature)}} - \underbrace{\frac{\partial w}{\partial s}}_{\text{(rotational displacement of straight beam)}}, \tag{3}$$

and W is independent of z and is completely defined by the centre-line component w . The relation for total circumferential strain is:

$$e_s = \frac{1}{\left(1 + \frac{z}{R}\right)} (\epsilon_s + z\beta_s), \tag{4}$$

where the in-plane (extensional) strain is given by

$$\epsilon_s = \underbrace{\frac{w}{R}}_{\text{(stretching due to radial displacement)}} + \underbrace{\frac{\partial u}{\partial s}}_{\text{(stretching due to motion in circumferential direction)}}, \tag{5}$$

and the bending strain (mid-surface change in curvature) is given by

$$\beta_s = \frac{\partial \phi}{\partial s}, \tag{6}$$

$$= \frac{\partial}{\partial s} \left(\frac{u}{R} - \frac{\partial w}{\partial s} \right). \tag{7}$$

See Appendix A for a complete derivation of the strain displacement expression. Since the radial stress component σ_r is assumed negligible, the transverse strain ϵ_r is zero, and as a consequence of Kirchoff's hypothesis the transverse shear strain

γ_{sr} is zero. Assuming the material to be linearly elastic, the circumferential stress-strain relationship is given by Hooke's Law:

$$\sigma_s = E\varepsilon_s, \quad (8)$$

where E is Young's modulus. Assuming the material to be homogeneous and isotropic, the material properties E , G and ν can be treated as constants. Thus, by integrating the stresses over the beam thickness, force and moment resultants are obtained. Using the strain-displacement expression, equation (4), the circumferential force is given by

$$N = ES \left(\frac{w}{R} + \frac{\partial u}{\partial s} \right) + \frac{EI}{R} \left(\frac{w}{R^2} + \frac{\partial^2 w}{\partial s^2} \right), \quad (9)$$

where S is the cross-sectional area of the beam, and I is the second moment of area of the cross-section. The bending moment is given by

$$M = -EI \left(\frac{w}{R^2} + \frac{\partial^2 w}{\partial s^2} \right). \quad (10)$$

Although the transverse shear stress σ_{sr} is zero, a non-vanishing shear resultant, Q , is defined as the integral across the thickness of the transverse shear stress, which leads to the following expression:

$$Q = -EI \frac{\partial}{\partial s} \left(\frac{w}{R^2} + \frac{\partial^2 w}{\partial s^2} \right). \quad (11)$$

Figure 2 shows the sign convention of force resultants on an elemental slice of a curved beam.

Flügge based equations of motion for a curved beam can be obtained by a reduction of the equations of motion for a circular cylindrical shell presented in reference [3]. This leads to the following set of equations:

$$RE \left(\frac{\partial^2 u}{\partial s^2} + \frac{1}{R} \frac{\partial w}{\partial s} \right) = \rho R \frac{\partial^2 u}{\partial t^2}, \quad (12)$$

$$-EK^2 R \frac{\partial}{\partial s^2} \left(\frac{w}{R^2} + \frac{\partial^2 w}{\partial s^2} \right) - \left[E \left(\frac{\partial u}{\partial s} + \frac{w}{R} \right) + \frac{EK^2}{R} \left(\frac{w}{R^2} + \frac{\partial^2 w}{\partial s^2} \right) \right] = \rho R \frac{\partial^2 w}{\partial t^2}, \quad (13)$$

where ρ is the density of the material, and K the radius of gyration. To obtain an harmonic solution assume that flexural and extensional sinusoidal waves propagate in the positive circumferential direction and can be represented respectively by:

$$w(s, t) = A \exp[i(\omega t - ks)], \quad (14)$$

$$u(s, t) = B \exp[i(\omega t - ks)], \quad (15)$$

where A and B are the complex wave amplitudes. Substituting these expressions into the equations of motion (12) and (13) gives the harmonic form of the

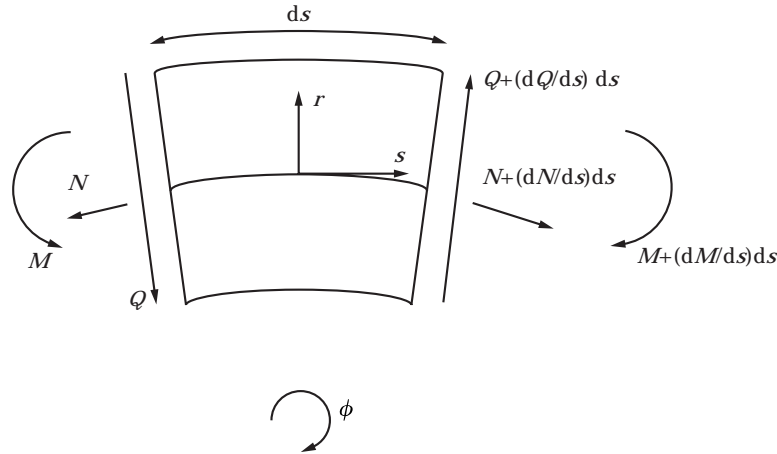


Figure 2. Sign convention and force resultants on an elemental slice of curved beam.

equations of motion:

$$\left[\frac{Ek^2}{\rho} - \omega^2 \right] B + i \frac{kE}{R\rho} A = 0, \tag{16}$$

$$-\frac{Eik}{R\rho} B + \left[\left(k^2 - \frac{1}{R^2} \right)^2 \frac{EK^2}{\rho} + \frac{E}{R^2\rho} - \omega^2 \right] A = 0. \tag{17}$$

2.2. NUMERICAL EXAMPLE

For a given radian frequency, ω , the harmonic equations of motion were solved to find the complex valued wave number, k , and corresponding wave amplitude ratio B/A . The physical dimensions and material properties were chosen to be the same as the mild steel beam used for the laboratory experiments. The physical properties of the beam are listed in Table 1. Wave number versus frequency curves for the beam are shown in Figure 3. The frequency range is expressed in terms of the non-dimensional frequency $\Omega = \omega R/c_o$, where c_o is the phase velocity of extensional waves in a straight bar, whilst the wave number range is expressed in terms of the non-dimensional wave number kR . The frequency axis extends over the non-dimensional frequency range $\Omega = 0.01$ to 10.0 which represents a dimensional frequency of 8.2 to 8200 Hz. It can be seen in Figure 3 that there are two different frequency regimes separated by the ring frequency $\Omega = 1$. Above the ring frequency the three wave types are: (i) a predominantly flexural travelling wave (marked with the symbol “*”); (ii) a predominantly flexural near field wave (marked with the symbol “○”); and (iii) a predominantly extensional travelling wave (marked with the symbol “+”). It can be seen in Figure 3 that above the ring frequency both flexural travelling waves and flexural near-field waves have the same wave number. Below the ring frequency the predominantly flexural travelling wave and the predominantly flexural near field waves still exist, however, the

TABLE 1

Physical properties of the experimental beam

Density, ρ (kg/m ³)	7850
Young's modulus, E (N/m ²)	207×10^9
Radius of curvature, R (m)	1.0
Breadth, b (m)	0.05
Depth, d (m)	6.068×10^{-3}

predominantly extensional travelling wave is now replaced by a predominantly extensional near field wave (marked with the symbol “×”). Below $\Omega = 0.1$ the predominantly flexural travelling and near field wave numbers diverge, with the travelling wave having the higher wave number.

2.3. RESPONSE DUE TO CIRCUMFERENTIAL EXCITATION AT THE FREE END

Assume that a “semi-infinite” beam with curvature is excited at its end by a point harmonic force, $F_s e^{i\omega t}$, acting in the circumferential direction, as shown in Figure 4. At a given position along the beam the total flexural or extensional displacement will be given by the sum of the displacements of the individual waves travelling away from the end of the beam. Thus, the total flexural displacement is given by

$$w(s) = A_1 e^{-ik_1 s} + A_2 e^{-ik_2 s} + A_3 e^{-ik_3 s}, \quad (18)$$

where A_1 , A_2 and A_3 represent the unknown wave amplitudes and k_1 , k_2 and k_3

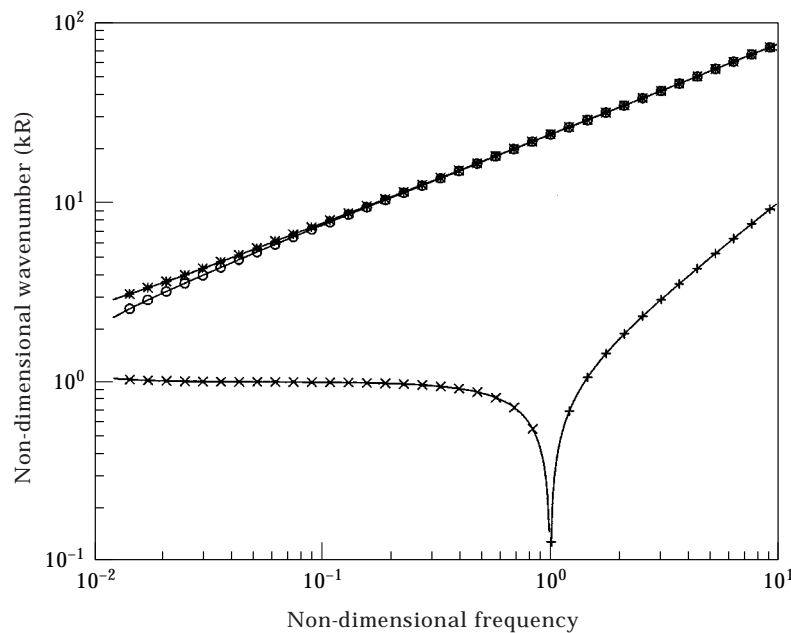


Figure 3. Wave number versus frequency relationship for a beam with a constant radius of curvature: *, predominantly flexural travelling wave; O, predominantly flexural near field wave; +, predominantly extensional travelling wave; ×, predominantly extensional near field wave.

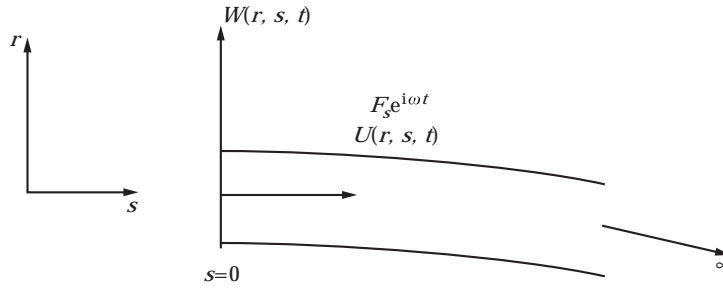


Figure 4. Diagram of the tangential displacement, U , and radial displacement, W , in a “semi-infinite” beam with curvature when excited by an harmonic force, $F_s e^{i\omega t}$, acting in the circumferential direction at the free end.

the respective wave numbers. For clarity of notation the harmonic term $e^{i\omega t}$ has been omitted. The corresponding extensional displacement is given by

$$u(s) = B_1 e^{-ik_1s} + B_2 e^{-ik_2s} + B_3 e^{-ik_3s}, \tag{19}$$

To determine the response of the structure the boundary conditions and applied load at the free end of the beam need to be evaluated. The boundary conditions and applied loads at $s = 0$ are: (i) that the axial force resultant is equal to the externally applied force; (ii) that the bending moment is zero; and (iii) that the shear force is zero. Substituting the displacement equations (18) and (19) into the Flügge based expressions for the resultant forces gives a set of three simultaneous equations in the unknown wave amplitudes A_1 , A_2 and A_3 . For a given excitation frequency, ω , the Flügge based equations of motion can be solved to find the three possible wave numbers, k_1 , k_2 and k_3 and the respective extensional to flexural wave amplitude ratios, B_i/A_i . Assuming a “semi-infinite” beam with waves travelling away from the excitation at the free end, then only three wave amplitudes ($A_1:A_2:A_3$) remain unknown. Substituting the previously calculated wave numbers, k_i into the set of three simultaneous equations and assuming unit force $F_s = 1$, enables the unknown wave amplitude ratios ($A_1:A_2:A_3$) to be evaluated. The cross receptance can now be calculated by evaluating the flexural displacement (equation (18)) at the excitation location:

$$\alpha_{zF} = \frac{w(0)}{F} = \frac{A_1 + A_2 + A_3}{F}. \tag{20}$$

Using the extensional to flexural wave amplitude ratios B_i/A_i , the point receptance can be calculated by evaluating the extensional displacement at the excitation location:

$$\alpha_{sF} = \frac{u(0)}{F} = \frac{B_1 + B_2 + B_3}{F}. \tag{21}$$

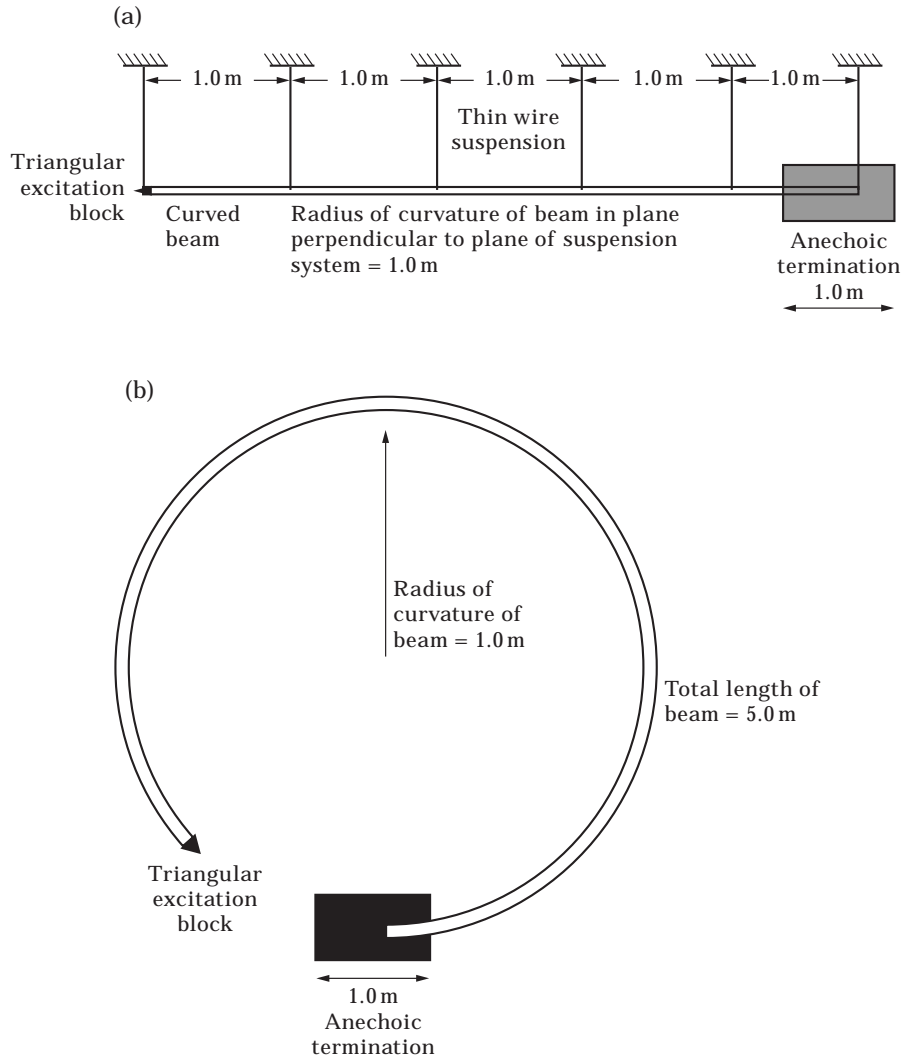


Figure 5. Schematic representation of the experimental apparatus: (a) side view, (b) top view.

3. EXPERIMENTAL APPARATUS AND METHOD

Figure 5 shows a schematic representation of the experimental curved beam. To obtain free conditions at the end of the beam, the whole beam was suspended on thin wires at 1-m intervals from underneath laboratory benches. It was assumed that no motion would occur in the plane of the suspension system. To obtain “semi-infinite” conditions one end of the beam was inserted into an anechoic termination. This termination consisted of a 1-m long box filled with sand to dissipate the energy of the wave motion. The excitation force was obtained by striking the beam with an instrumented hammer (BK8202) at the free end. To assist in obtaining a purely circumferential force a hard steel triangular block was glued at the centre of the cross-section of the free end of the beam. The applied force was measured with the instrumented hammer,

whilst the response acceleration was measured using two 11-g accelerometers (BK4371). Extensional motion was measured using an accelerometer mounted on the cross-section of the beam just above the triangular block and, flexural motion was measured using an accelerometer, mounted on the centre-line of the side of the beam. The applied force and resulting accelerations were recorded simultaneously on an HP3566A spectrum analyser and the point and cross mobility calculated directly from a single measurement by dividing the Fourier transform of the response velocity by that of the applied force.

The instrumented hammer provides an excitation force with a significant frequency spectrum up to approximately 10 kHz with a usable frequency range (below the first zero) up to approximately 3 kHz. Thus, for the frequency response measurements anti-alias filters within the spectrum analyser were set at 3200 Hz, and a sampling rate of 8192 samples/s chosen, giving a folding frequency of 4096 Hz. To record the entire decaying response a Fast Fourier Transform (FFT) block size of 8192 points was chosen, giving a record length of 1 s, and a frequency resolution of 1 Hz. The digitised time histories were transformed to the frequency domain using an FFT algorithm within the spectrum analyser. Since the time histories were recordings of transient signals, the rectangular data window was chosen. The spectra of the acceleration signals were integrated in the frequency domain by division by $i\omega$, and the point and cross mobilities calculated from a single measurement by complex division of the respective velocity spectra by the excitation force spectrum. The mobility data shown in Figures 6 and 7 are presented on non-dimensional frequency axes. These were obtained from the dimensional spectra by multiplying the frequency axis by $2\pi R/c_o$.

4. RESULTS

The predicted point mobility is compared with the measured point mobility in Figure 6 over the non-dimensional frequency range $\Omega = 0.01$ to 10.0 . Figure 6(a) shows the modulus of the point mobility which indicates that there are two frequency regions separated by the ring frequency $\Omega = 1.0$. Above the ring frequency the predicted value of the point mobility (marked with “○” symbols) asymptotes to a constant value of 8×10^{-5} (m/s)/N as the frequency increases. This value corresponds to the point mobility of purely extensional waves in a “semi-infinite” straight bar given by reference [10] as

$$Y_s F = \frac{c_o}{ES}. \quad (22)$$

The corresponding measured data show resonant behaviour, with the resonant frequencies corresponding approximately to those of purely extensional waves in a straight rod of length 5 m, with the same material properties as the experimental curved beam.

Below the ring frequency extensional near-field waves are to be expected rather than travelling extensional waves. This is confirmed by inspection of the modulus of the point mobility shown in Figure 6(a) where it can be seen that the

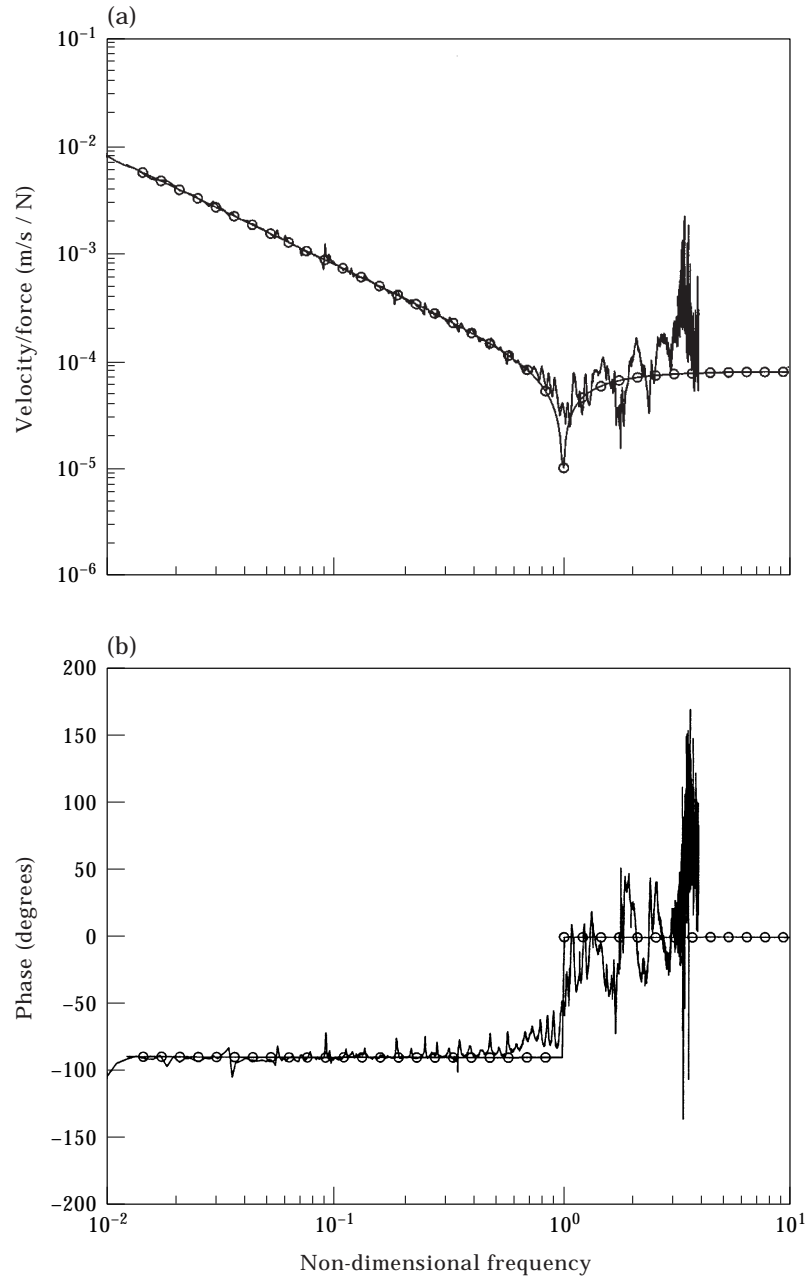


Figure 6. (a) Modulus of the point mobility and (b) phase angle of the point mobility (i.e., resulting extensional velocity/circumferentially acting force) of the experimental curved beam when excited by a force acting at the free end (predicted data marked with "O" symbols).

experimental data do not exhibit resonant behaviour. Both the measured and predicted data exhibit the characteristics of a "mass line" and it is shown in Appendix B that below the ring frequency the beam acts as a mass of length equal to the radius of curvature, R . Further, in terms of the non-dimensional frequency, Ω , the point mobility can be expressed as

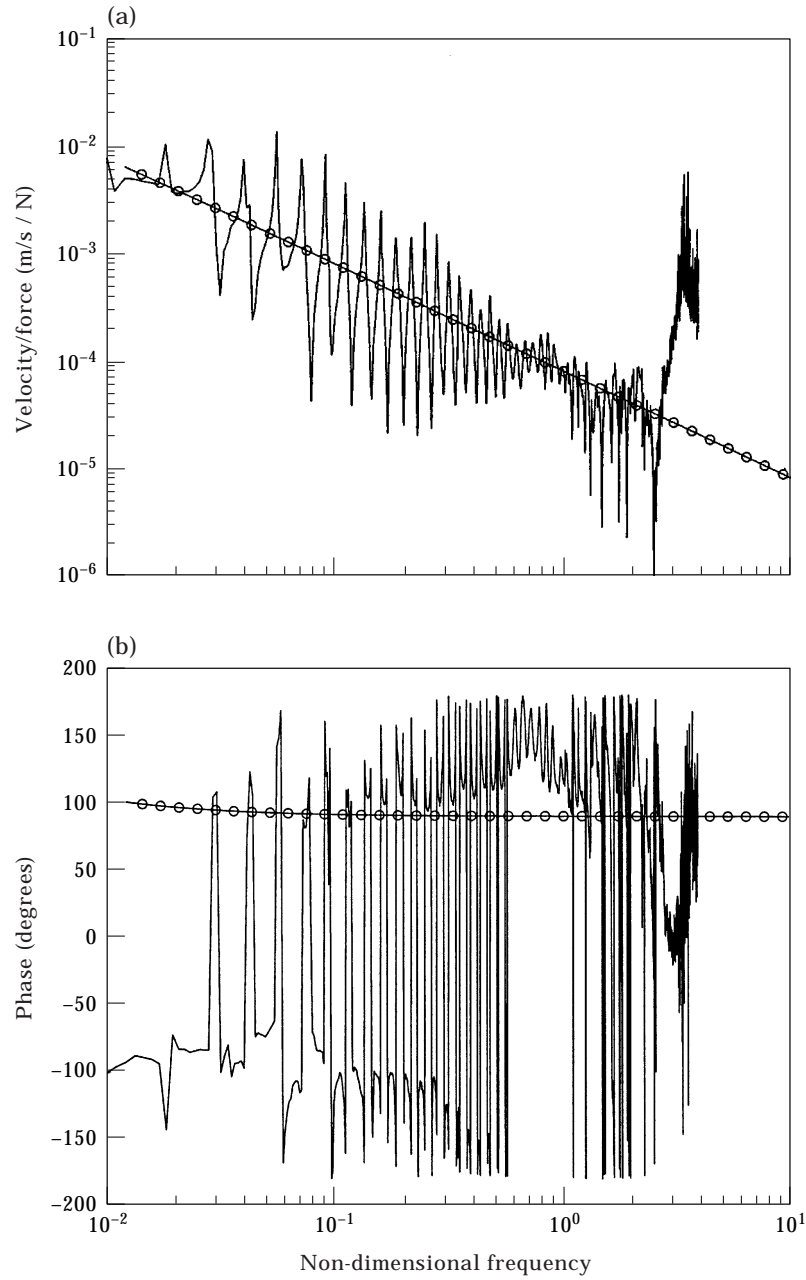


Figure 7. (a) Modulus of the cross mobility and (b) phase angle of the cross mobility (i.e., resulting flexural velocity/circumferentially acting force) of the experimental curved beam when excited by a force acting at the free end (predicted data marked with “○” symbols).

$$Y_{sF} = \frac{-i}{\Omega S \rho c_o}. \quad (23)$$

Figure 6(b) shows the corresponding phase angle which indicates that below the ring frequency the velocity is 90° out of phase with force and thus only near field waves are being generated. Above the ring frequency the velocity is in phase with the applied force and, thus travelling waves are being generated.

Figure 7 shows the measured and predicted cross mobility (flexural velocity per unit circumferential force). The modulus is shown in Figure 7(a) where the measured data indicate resonant behaviour with the measured resonant frequencies corresponding approximately to the natural frequencies due to flexural waves in a free-free beam of length 5 m. This is surprising as the point mobility indicated that the response consists largely of near field extensional waves below the ring frequency, and thus the measured data should not exhibit resonant behaviour. This discrepancy may be due to the wave length of the extensional near field waves being greater than the length of the experimental beam (5 m). Thus, at the end of the beam within the anechoic termination the predominantly extensional waves may be converted into predominantly flexural travelling waves which gives rise to the resonant behaviour shown in Figure 7. Comparison of the predicted modulus of the cross mobility shown in Figure 7(a) with the predicted modulus of point mobility shown in Figure 6(a) indicates that both functions have the same value below the ring frequency. Comparison of the phase angle of the cross mobility shown in Figure 7(b) with the phase angle of the point mobility shown in Figure 6(b) indicates a 180° phase difference between the phase angle of the cross mobility and the phase angle of the point mobility below the ring frequency. Thus, from equation (23) the cross mobility is given by

$$Y_{zF} = \frac{i}{\Omega S \rho c_o}. \quad (24)$$

In terms of radian frequency, ω , this becomes

$$Y_{zF} = \frac{i}{\omega R S \rho}. \quad (25)$$

Thus, from equation (25) it can be seen that the cross mobility is dependent upon the frequency, ω , the radius of curvature, R , and the mass per unit length, $S\rho$, of the beam. It can also be seen that the flexural velocity is 90° out of phase with the applied circumferential force.

5. SUMMARY

In this paper both measured and predicted levels of the mobility of a “semi-infinite” beam with a constant radius of curvature have been presented, the beam being excited in the circumferential direction at the free end. The results of

this study can be summarised as follows: (a) The point mobility has two frequency regions separated by the ring frequency. Above the ring frequency the point mobility is dominated by predominantly extensional travelling waves and has a constant value which asymptotes to the point mobility of purely extensional waves in a straight “semi-infinite” bar. Below the ring frequency the point mobility is dominated by predominantly extensional near field waves and the beam acts as a mass of length equal to the radius of curvature. (b) The cross mobility is dependant upon frequency, the radius of curvature and the mass per unit length of the beam. The flexural velocity is 90° out of phase with the applied circumferential force.

ACKNOWLEDGMENTS

The experimental work was undertaken at the Institute of Sound and Vibration Research, University of Southampton.

REFERENCES

1. A. E. H. LOVE 1940 *A Treatise on the Mathematical Theory of Elasticity* New-York: Dover Publications.
2. T. E. LANG 1962 *Jet Propulsion Laboratory Technical Report*, 32–261. Vibration of thin circular rings.
3. A. W. LEISSA 1977 *Vibrations of Shells*. NASA SP-288, Washington, D.C.
4. L. L. PHILIPSON 1956 *Journal of Applied Mechanics* **23**, 364–366. On the role of extension in the flexural vibrations of rings.
5. L. S. D. MORLEY 1961 *Quarterly Journal of Mechanics and Applied Mathematics* **14**, 155–172. Elastic waves in a naturally curved rod.
6. K. F. GRAFF 1975 *Wave Motion in Elastic Solids*. Oxford: Clarendon Press.
7. K. F. GRAFF 1970 *IEEE Transactions of Sonics and Ultrasonics* **SU-17**, 1–16. Elastic wave propagation in a curved sonic transmission line.
8. D. J. MEAD 1986 *Journal of Sound and Vibration* **104**, 9–27. A new method of analysing wave motion in periodic structures: applications to periodic Timoshenko beams and stiffened plates.
9. D. J. MEAD 1990 *Journal of Sound and Vibration* **141**, 465–484. The harmonic response of uniform beams on multiple linear supports: a flexural wave analysis.
10. L. CREMER, M. HECKL and E. E. UNGAR 1973 *Structure-Borne Sound*. Berlin: Springer.
11. E. SKUDRZYK 1968 *Simple and Complex Vibratory Systems*. Pennsylvania State University Press.

APPENDIX A: DERIVATION OF CIRCUMFERENTIAL STRAIN IN TERMS OF COMPONENTS OF DISPLACEMENT AT THE UNDEFORMED CENTRE-LINE

By considering the deformation of an element of a circular cylindrical shell Cremer *et al.* [10] derive an expression for total circumferential strain [10, p. 177] which can be written as

$$e_s = \frac{1}{\left(1 + \frac{z}{R}\right)} \left(\frac{W}{R} + \frac{\partial U}{\partial s} \right), \quad (\text{A1})$$

where the tangential and radial displacements of the material point are $U(r, s, t)$ and $W(r, s, t)$, respectively. For small displacements of thin beams the assumptions known as ‘‘Love’s first approximation’’, in classical shell theory, can be made which leads to the following linear relationships between the displacements of a material point and components of displacement at the undeformed centre-line

$$U(r, s, t) = u(R, s, t) + z\phi(s, t), \quad (1)$$

$$W(r, s, t) = w(R, s, t), \quad (2)$$

where u and w are the components of displacement at the centre-line in the tangential and radial directions, respectively and, ϕ is the rotation of the normal to the centre-line during deformation

$$\phi = \underbrace{\frac{u}{R}}_{\text{(angle of curvature)}} - \underbrace{\frac{\partial w}{\partial s}}_{\text{(rotational displacement of straight beam)}}, \quad (3)$$

and W is independent of z and is completely defined by the centre-line component w . Substituting equations (1) and (2) into the strain–displacement equation (A1) gives the following relation for total circumferential strain

$$e_s = \frac{1}{\left(1 + \frac{z}{R}\right)} \left(\frac{w}{R} + \frac{\partial u}{\partial s} + z \frac{\partial \phi}{\partial s} \right). \quad (\text{A2})$$

This can be expressed as

$$e_s = \frac{1}{\left(1 + \frac{z}{R}\right)} (\varepsilon_s + z\beta_s), \quad (4)$$

where the in-plane (extensional) strain is given by

$$\varepsilon_s = \underbrace{\frac{w}{R}}_{\text{(stretching due to radial displacement)}} + \underbrace{\frac{\partial u}{\partial s}}_{\text{(stretching due to motion in circumferential direction)}}, \quad (5)$$

and the bending strain (mid-surface change in curvature) is given by

$$\beta_s = \frac{\partial \phi}{\partial s}, \quad (6)$$

$$= \frac{\partial}{\partial s} \left(\frac{u}{R} - \frac{\partial w}{\partial s} \right). \quad (7)$$

APPENDIX B: DERIVATION OF THE POINT MOBILITY BELOW THE RING FREQUENCY OF A "SEMI-INFINITE" BEAM WITH CONSTANT CURVATURE EXCITED BY A FORCE ACTING IN THE CIRCUMFERENTIAL DIRECTION AT THE FREE END

The mobility of a simple mass element is given by reference [11] as

$$Y = \frac{-i}{\omega m}. \quad (B1)$$

In terms of the non-dimensional frequency, Ω , this can be expressed as

$$Y = \frac{-iR}{\Omega c_o m}. \quad (B2)$$

In Figure 6(a) the modulus of the mobility at $\Omega = 1.0$ is at the intersection with the point mobility of travelling extensional waves. Thus,

$$\begin{aligned} |Y| &= \frac{R}{\Omega c_o m} \\ &= 8.067 \times 10^{-5} \text{ (m/s)/N}. \end{aligned} \quad (B3)$$

Therefore, $m = 2.414 R$. But, the mass per unit length of the beam $S\rho = 2.414$ (kg). Hence, below the ring frequency the beams act as a mass of length equal to the radius of curvature. Further, substituting for the mass, $m = SR\rho$, into equation (B1) gives an expression for the point mobility below the ring frequency:

$$Y = \frac{-i}{\omega SR\rho}. \quad (B4)$$

In terms of the non-dimensional frequency, Ω , this becomes

$$Y = \frac{-i}{\Omega S\rho c_o}. \quad (B5)$$

APPENDIX C: NOTATION

- A* flexural wave amplitude
- B* extensional wave amplitude
- E* Young's modulus
- F_s* magnitude of externally applied force acting in circumferential direction

G	shear modulus
I	second moment of area of cross-section of beam
K	radius of gyration
M	bending moment on cross-section of beam
N	circumferential force on cross-section of beam
Q	shear force on cross-section of beam
R	radius of curvature
S	cross-sectional area of beam
U	displacement of material point in circumferential direction
W	displacement of material point in radial direction
Y	mobility
b	breadth (width) of beam
c_o	wavespeed of extensional waves in a straight bar
e_s	total circumferential strain
h	thickness of beam
k	wavenumber
m	mass
r	co-ordinate in radial direction
s	co-ordinate in circumferential direction
t	time
u	displacement at centre-line in circumferential direction
w	displacement at centre-line in radial direction
z	co-ordinate of outward pointing normal
Ω	non-dimensional frequency
α	receptance
β_s	bending strain
γ_{sr}	transverse shear strain
ε_r	radial strain
ε_s	circumferential strain
ν	Poisson's ratio
ρ	density
σ_r	radial stress
σ_s	circumferential stress
σ_{sr}	transverse shear stress
ϕ	change in slope of normal to centre-line during deformation
ω	radian frequency